molecules

MDPI

Article

Au Modified F-TiO_2 for Efficient Photocatalytic Synthesis of Hydrogen Peroxide

Lijuan Li [1,†], Bingdong Li [1,†], Liwei Feng [1,†], Xiaoqiu Zhang [2], Yuqian Zhang [1], Qiannan Zhao [1], Guifu Zuo [1] and Xianguang Meng [1,*]

[1] Hebei Provincial Laboratory of Inorganic Nonmetallic Materials, College of Materials Science and Engineering, North China University of Science and Technology, Tangshan 063210, China; Lilj5527@163.com (L.L.); libingdong1226@163.com (B.L.); 13473519550@163.com (L.F.); 18332737639@163.com (Y.Z.); 18332725160@163.com (Q.Z.); zuoguifu@163.com (G.Z.)

[2] Chemistry Group, No.2 Experimental Middle School of Dehui, Dehui 130300, China; zhangxiaoqiu-913@163.com

* Correspondence: mengxg_materchem@163.com

† These authors contributed equally to this work.

Abstract: In this work, Au-modified F-TiO_2 is developed as a simple and efficient photocatalyst for H_2O_2 production under ultraviolet light. The Au/F-TiO_2 photocatalyst avoids the necessity of adding fluoride into the reaction medium for enhancing H_2O_2 synthesis, as in a pure TiO_2 reaction system. The F^- modification inhibits the H_2O_2 decomposition through the formation of the ≡Ti–F complex. Au is an active cocatalyst for photocatalytic H_2O_2 production. We compared the activity of TiO_2 with F^- modification and without F^- modification in the presence of Au, and found that the H_2O_2 production rate over Au/F-TiO_2 reaches four times that of Au/TiO_2. In situ electron spin resonance studies have shown that H_2O_2 is produced by stepwise single-electron oxygen reduction on the Au/F-TiO_2 photocatalyst.

Keywords: photocatalysis; hydrogen peroxide; fluorination; TiO_2

check for updates

Citation: Li, L.; Li, B.; Feng, L.; Zhang, X.; Zhang, Y.; Zhao, Q.; Zuo, G.; Meng, X. Au Modified F-TiO_2 for Efficient Photocatalytic Synthesis of Hydrogen Peroxide. *Molecules* **2021**, *26*, 3844. https://doi.org/10.3390/molecules26133844

Academic Editor: Giuseppina Pinuccia Cerrato

Received: 14 May 2021
Accepted: 17 June 2021
Published: 24 June 2021

1. Introduction

Hydrogen peroxide (H_2O_2) is widely used as a clean oxidant in environmental purification and organic synthesis [1,2]. It is widely used in pulp bleaching, wastewater treatment, and disinfection of industrial and household wastes with only water as the by-product [3]. At present, most H_2O_2 in industry is prepared by the anthraquinone method with H_2 and O_2 [4]. This method requires a lot of energy and organic solvents with complicated reaction steps and high risk of explosion. Therefore, finding a simple and direct method for H_2O_2 synthesis has become the focus of research. H_2O_2 can be effectively produced through photo-electrocatalysis [5] and photocatalysis. In recent years, the photocatalytic synthesis of H_2O_2 with oxygen and sunlight as the input energy has attracted great attention. At present, many semiconductor materials with UV and visible light activities, such as ZnO [6,7], C_3N_4 [8–10], $BiVO_4$ [11], and TiO_2 [12–18] have demonstrated the potential for direct synthesis of H_2O_2. Especially when these semiconductors are loaded with appropriate cocatalysts, the photocatalytic activity of the catalysts could be greatly improved. Au has been proved to be a very effective cocatalyst for promoting H_2O_2 production.

As a classic photocatalyst, TiO_2 is one of the most frequent and promising semiconductors because of its low cost and high stability. Under UV irradiation, H_2O_2 can be directly produced in aqueous solution in the presence of O_2 without hydrogen over TiO_2. An important feature of photocatalytic H_2O_2 synthesis is that the formation of H_2O_2 from the oxygen reduction reaction (ORR) is accompanied by the decomposition process. Zhao et al. [19] reported that adsorption of H_2O_2 on TiO_2 will readily form surface peroxide complexes in the form of ≡Ti–OOH, which can be easily photodegraded with a zero-order kinetic process, even with the irradiation of visible light, thus leading to the decrease in H_2O_2 production. Maurino et al. [20] also reported that the production of H_2O_2 increased remarkably after adding fluoride into the reaction suspension of TiO_2. These studies showed the competition of the F^- with superoxide/peroxide species for the surface sites of TiO_2. The ≡Ti–F formation decreases the amount of ≡Ti–OOH and thus, inhibits H_2O_2 degradation. This method is interesting but it will cause fluoride pollution to the reaction medium and the difficulty of H_2O_2 purification. In order to solve these problems, we developed F^--modified TiO_2 by a hydrothermal method instead of adding NaF in the photocatalytic reaction medium and used Au as the cocatalyst of F-TiO_2. The anchored F^- on the TiO_2 surface will compete with the formation of peroxide species to suppress the decomposition of H_2O_2 and increase the H_2O_2 production rate. F-TiO_2 avoided adding fluoride into the reaction medium as used in a pure TiO_2 reaction system and thus, simplified the reaction procedure. In situ ESR reveals that the H_2O_2 is efficiently formed through a stepwise single-electron ORR process on the Au/F-TiO_2 photocatalyst.

2. Materials and Methods

2.1. Experimental Materials Preparation

To produce the F-TiO_2 photocatalyst, 1 g commercial anatase TiO_2 and 0.42 g NaF (n_F:n_{Ti} = 0.5:1) were mixed with 25 mL absolute ethanol and 15 mL water for hydrothermal treatment. The powder mixtures were maintained at 180 °C for 4 h in a homogeneous reactor. Then, the mixtures were transferred into the deionized water for centrifugation, washing and drying. By changing the amount of NaF and TiO_2 with different molar ratios of F/Ti, we prepared a series of F-TiO_2 photocatalysts. The photocatalysts loaded with 0.1 wt% Au were obtained by the deposition–precipitation method reported previously [21].

2.2. Material Characterization

UV–Vis spectra were recorded with a Spectrum Lambda 750 S (Perkin-Elmer, Waltham, MA, USA). High-resolution transmission electron microscopy (TEM) characterization was performed with an 8000EX microscope (JEOL, Tokyo, Japan) operating at 200 kV. The S-4800 scanning electron microscope (SEM) from Hitachi Instruments was used to observe the morphology of the photocatalyst.

2.3. Photocatalytic Activity Test

A reaction kettle (200 mL) was used as a photocatalytic reactor; 0.2 g Au/F-TiO_2 was added into the reaction solution of alcohol (4 wt%) and deionized water. F^- was directly modified on the surface of the TiO_2 by the hydrothermal method without adding F^- into the reaction solution. The suspension was treated by ultrasonication for 2–3 min; then, oxygen was bubbled for 30 min before turning on the light. A 300 W Xe arc lamp (PLS-SXE300, Perfectlight Technology Co., Ltd., Beijing, China) was used as a light source. The reaction was carried out under magnetic stirring water cooling. The concentrations of H_2O_2 generated were determined by using the DMP (2, 9-dimethyl-1, 10-phenanthroline) method [22].

2.4. Quantification of H_2O_2 (DMP Method)

One milliliter of DMP (0.1 g/L), 1 mL of copper (II) sulfate (0.1 M), 1 mL of phosphate buffer (Ph 7.0) solution, and 1 mL of reaction solution were added to a 10 mL volumetric flask and mixed; then, deionized water was added to the volumetric flask to the tick mark. After mixing, the absorbance of the sample at 454 nm was measured. The blank solution was prepared in the same manner but without H_2O_2.

The concentrations of H_2O_2 were calculated by the following formula:

$$A_{454} = \zeta\,[H_2O_2] \times 1/10$$

where A_{454} is the difference of the absorbance between the sample and blank solutions at 454 nm, ζ is the slope of the calibration curve, and $[H_2O_2]$ is the H_2O_2 concentration (μM).

2.5. In Situ ESR Test

Using 5,5-dimethyl-1-pyrroline N-oxide (DMPO) as spin trapping reagent, the reduction pathways of O_2 on different catalysts were determined by in situ electron spin resonance (ESR) analysis. An ESP 300E spectrometer (Bruker, Switzerland) was used to detect the ESR signals of radicals trapped by DMPO. Generally, the catalyst (1 mg) was put into a mixture containing 1 mL alcohol/water (4 wt%) and 0.125 mmol DMPO. After passing the O_2 for 3 min, the sample was irradiated under UV light for 5 min before testing.

3. Results and Discussion

Au/TiO_2 and TiO_2 have similar XRD test spectra (Figure S1). The diffraction peak of Au was not observed. It is presumed that the content of Au is too low and it is highly dispersed in the catalyst, which makes it impossible to form obvious characteristic diffraction peaks. In order to explore the existence and state of F^- in the catalyst, the XPS of Au/TiO_2 and Au/F-TiO_2 was tested (Figure S2). Compared with the full spectrum of Au/TiO_2, the full spectrum of Au/F-TiO_2 has a peak corresponding to F1s between 600 eV and 700 eV, which can preliminarily prove that F^- has been successfully introduced into the catalyst. From the peak fitting results of the high-resolution XPS spectrum of F1s (Figure 1), it is found that the F1s is mainly composed of two peaks. The low binding energy peak at 683.4 eV is the signal peak of the formation of complex ≡Ti-F due to the chemical adsorption of F^- on the surface of TiO_2. The small peak with high binding energy near 684.5 eV is attributed to the signal peak of the doped F atom in TiO_2; that is, the F atom substituting for the oxygen site in TiO_2 lattice.

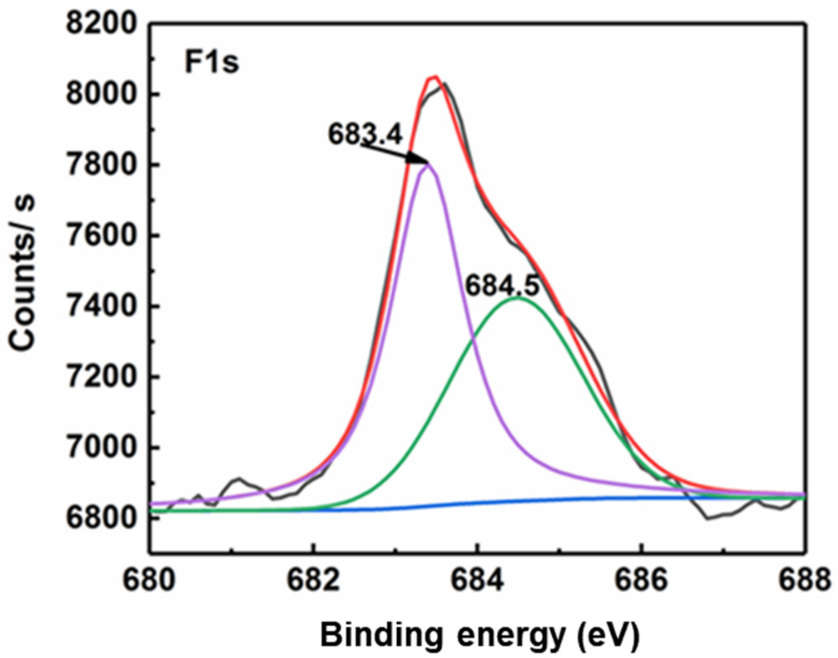

Figure 1. High-resolution XPS spectrum of F1s.

From the TEM image of TiO_2 and F-TiO_2 (Figure 2), it is found that the morphology of F-TiO_2 prepared by the hydrothermal method has a very obvious change compared with that of TiO_2. TiO_2 has an irregular shape, while F-TiO_2 is almost spherical. This is because F^- has an etching effect on TiO_2 during hydrothermal treatment [23]. The F^- has a strong complexation ability with Ti on the surface of TiO_2, which corrodes the edges and corners of TiO_2 particles and changes the irregular TiO_2 into a spherical shape [24].

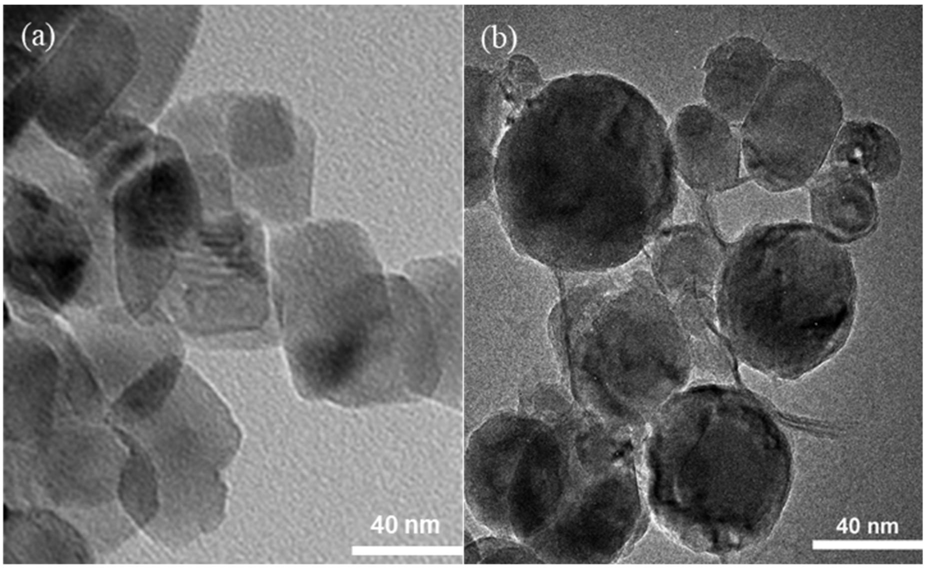

Figure 2. TEM images of (**a**) TiO_2 and (**b**) F-TiO_2.

The SEM and energy dispersive spectroscopy (EDS) of 0.1% Au/F-TiO_2 (Figure S3) show that there are F and Au elements on the surface of the catalyst. This also proved that the F^- modification and Au loading on TiO_2 were successfully realized in the sample preparation. The element mapping of Au/F-TiO_2 (n_F: n_{Ti} = 2.5) in Figure 3 shows that both F and Au are evenly distributed on the surface of TiO_2, which is consistent with the element types shown in the EDS result (Figure S3).

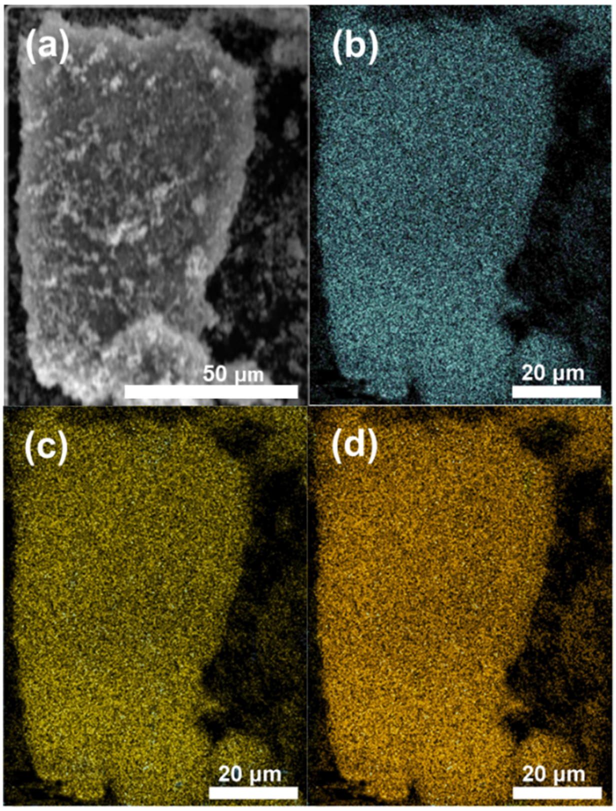

Figure 3. (**a**) SEM and mapping images of (**b**) Ti, (**c**) F and (**d**) Au elements on Au/F-TiO_2 (n_F:n_{Ti} = 2.5).

Figure 4a shows the UV–Vis spectrum of F-TiO_2, 0.1% Au/F-TiO_2 and pure TiO_2. Besides the characteristic absorption bands of TiO_2 at lower than 370 nm, the absorption bands caused by the loading of Au nanoparticles are located between 500 nm and 650 nm, which is a typical Au surface plasma band [25]. According to the calculation, the band gap of TiO_2 is about 3.2 eV and F-TiO_2 is about 3.1 eV (Figure 4b).

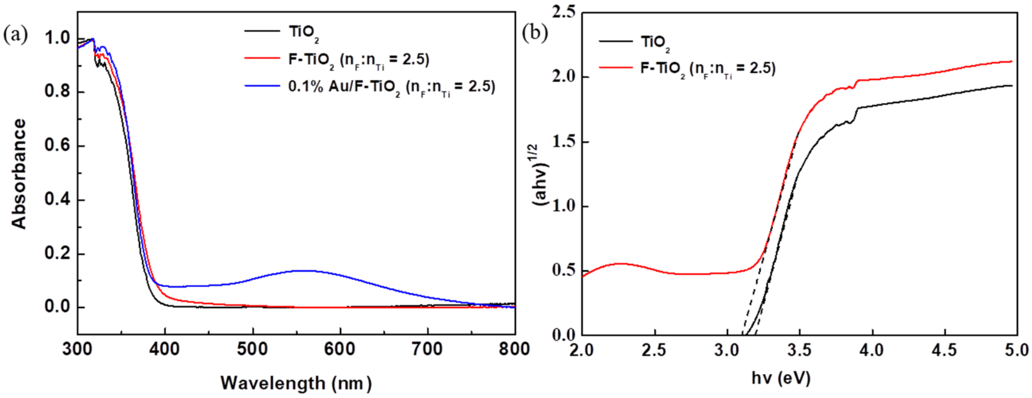

Figure 4. (**a**) UV–Vis absorbance from Kubelka–Munk function of diffuse–reflectance spectra of TiO_2, F-TiO_2 and 0.1% Au/F-TiO_2; (**b**) Tauc plot from (**a**).

The photocatalytic activity of H_2O_2 synthesis on Au/F-TiO_2 hybrids was tested under UV light and the concentration of H_2O_2 was quantified by spectrophotometry with copper ions and 2,9-dimethyl-1,10-phenanthroline (DMP). The standard curve showed that there was a good linear relationship between the absorbance and concentration of H_2O_2; the R squared value was 0.9996 (Figure S3). Figure 5 shows the photocatalytic synthesis of H_2O_2 over Au-loaded F-TiO_2 catalysts. Compared with the unmodified catalyst, the photocatalytic activity increased with the increase in F content, and the photocatalytic activity reached its highest when the F/Ti molar ratio increased to 2.5. The F^- on the surface of TiO_2 will compete with superoxide/peroxide species for the surface sites of TiO_2 and inhibit the adsorption of peroxy radicals, thus suppressing the decomposition of H_2O_2. With the continuous increase in F content, when the F/Ti molar ratio is 3, the activity of the catalyst decreases. Excessive F^- caused serious defects on the surface of TiO_2 and destroyed the crystallinity of TiO_2, thus decreasing the photocatalytic activity of the catalyst.

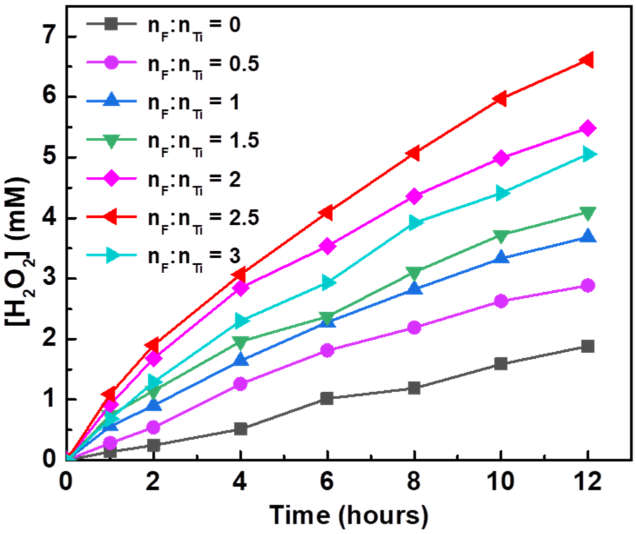

Figure 5. Photocatalytic H_2O_2 production over 0.1% Au/F-TiO_2 prepared with different F/Ti ratios.

In general, H_2O_2 from 2 e^- ORR by CB electrons can be produced through stepwise coupled electrons and proton transfers (Equations (1)–(3)) [26]. In order to further study the mechanism of photocatalytic ORR for H_2O_2 synthesis over Au/F-TiO_2, DMPO was used as a trapping agent of free radical in situ ESR tests for different samples. In situ ESR spectra of Au/F-TiO_2, Au/TiO_2 and pure TiO_2 under UV irradiation are shown in Figure 6. The results clearly show the signal of •OOH formed via equation (2) over various TiO_2 photocatalysts [27]. The DMPO-•OOH radical signal could be detected in both Au-loaded samples except pure TiO_2. The superoxide radical is formed by the first combination of O_2 in the photocatalytic reaction medium with electrons and protons. The generated HO_2• will continue to react with one electron and a proton and finally, generate H_2O_2. Therefore, the H_2O_2 is formed by a stepwise single-electron ORR over Au/F-TiO_2. In addition, compared with TiO_2, Au/TiO_2 and Au/F-TiO_2 produced a more obvious HO_2• signal, which implied that Au and F^- promoted the formation of HO_2•, and both of them promoted the photocatalytic synthesis of H_2O_2.

$$\text{Semiconductor} \rightarrow e^- + h^+ \tag{1}$$

$$e^- + O_2 + H^+ \rightarrow \bullet OOH \tag{2}$$

$$\bullet OOH + H^+ + e^- \rightarrow H_2O_2 \tag{3}$$

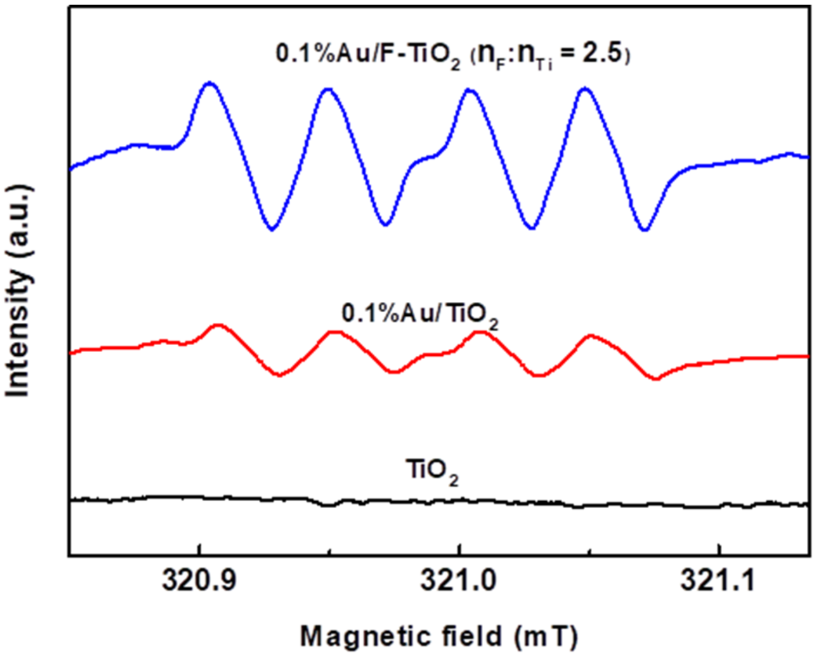

Figure 6. In situ ESR spectra of 0.1% Au/TiO_2 prepared with different F/Ti ratios and pure TiO_2.

4. Conclusions

In this work, we have designed Au/F-TiO_2 as an efficient photocatalyst for the production of H_2O_2 in aqueous solution. The Au/F-TiO_2 makes it possible to obtain a high H_2O_2 yield in fluoride-free reaction medium. The H_2O_2 production rate reached four times that of Au/TiO_2. The in situ ESR test showed that the synthesis mechanism of H_2O_2 was not changed by F^- modification. The H_2O_2 was synthesized over Au/F-TiO_2 through a stepwise single-electron ORR.

Supplementary Materials: The following are available online. Figure S1: XRD spectra of Au/TiO_2 and TiO_2, Figure S2: XPS spectra of (a) Au/TiO_2, (b) Au/F-TiO_2, Figure S3: (a) SEM image of 0.1%Au/F-TiO_2, (b) EDS spectrum of 0.1%Au/F-TiO_2, Figure S4: Standard curve: linear relationship between absorbance at 454 nm and H_2O_2 concentration.

Author Contributions: Conceptualization, X.M.; methodology, X.M.; software, L.L., B.L.; validation, X.M.; formal analysis, L.L., B.L., L.F., X.Z., G.Z. and X.M.; investigation, L.L., B.L., L.F., Y.Z., Q.Z. and G.Z.; resources, X.M.; data curation, L.L. and B.L.; writing—original draft preparation, L.L., L.F. and X.M.; writing—review and editing, X.M.; visualization, X.M.; supervision, X.M.; project administration, X.M.; funding acquisition, X.M. All authors have read and agreed to the published version of the manuscript.

Funding: This work was supported by the National Natural Science Foundation of China (51872091), "Hundred Talents Program" of Hebei Province (E2018050013), Natural Science Foundation of Hebei Province (B2018209267), and Outstanding Youth Funds of North China University of Sci-ence and Technology (JP201604 and JQ201706).

Institutional Review Board Statement: Not applicable.

Informed Consent Statement: Not applicable.

Acknowledgments: This work was supported by the National Natural Science Foundation of China (51872091), "Hundred Talents Program" of Hebei Province (E2018050013), Natural Science Foundation of Hebei Province (B2018209267), and Outstanding Youth Funds of North China University of Science and Technology (JP201604 and JQ201706).

Conflicts of Interest: The authors declare no conflict of interest.

Sample Availability: Not available.

References

1. Sato, K.; Aoki, M.; Noyori, R. A 'Green' Route to Adipic Acid: Direct Oxidation of Cyclohexenes with 30 Percent Hydrogen Peroxide. *Science* **1998**, *281*, 1646–1647. [CrossRef] [PubMed]
2. Samanta, C. Direct synthesis of hydrogen peroxide from hydrogen and oxygen: An overview of recent developments in the process. *Appl. Catal. A Gen.* **2008**, *350*, 133–149. [CrossRef]
3. Zuo, G.; Liu, S.; Wang, L.; Song, H.; Zong, P.; Hou, W.; Li, B.; Guo, Z.; Meng, X.; Du, Y.; et al. Finely dispersed Au nanoparticles on graphitic carbon nitride as highly active photocatalyst for hydrogen peroxide production. *Catal. Commun.* **2019**, *123*, 69–72. [CrossRef]
4. Moon, G.-H.; Kim, W.; Bokare, A.D.; Sung, N.-E.; Choi, W. Solar production of H2O2on reduced graphene oxide–TiO_2hybrid photocatalysts consisting of earth-abundant elements only. *Energy Environ. Sci.* **2014**, *7*, 4023–4028. [CrossRef]
5. Andrade, T.S.; Papagiannis, I.; Dracopoulos, V.; Pereira, M.C.; Lianos, P. Visible-Light Activated Titania and Its Application to Photoelectrocatalytic Hydrogen Peroxide Production. *Materials* **2019**, *12*, 4238. [CrossRef]
6. Kormann, C.; Bahnemann, D.W.; Hoffmann, M.R. Photocatalytic production of hydrogen peroxides and organic peroxides in aqueous suspensions of titanium dioxide, zinc oxide, and desert sand. *Environ. Sci. Technol.* **1988**, *22*, 798–806. [CrossRef]
7. Domènech, X.; Ayllón, J.A.; Peral, J. H2O2 formation from photocatalytic processes at the ZnO/water interface. *Environ. Sci. Pollut. Res.* **2001**, *8*, 285–287. [CrossRef]
8. Shi, L.; Yang, L.; Zhou, W.; Liu, Y.; Yin, L.; Hai, X.; Song, H.; Ye, J. Photoassisted Construction of Holey Defective g-C_3N_4 Photocatalysts for Efficient Visible-Light-Driven H_2O_2 Production. *Small* **2018**, *14*, 1703142. [CrossRef] [PubMed]
9. Shiraishi, Y.; Kanazawa, S.; Sugano, Y.; Tsukamoto, D.; Sakamoto, H.; Ichikawa, S.; Hirai, T. Highly Selective Production of Hydrogen Peroxide on Graphitic Carbon Nitride (g-C_3N_4) Photocatalyst Activated by Visible Light. *ACS Catal.* **2014**, *4*, 774–780. [CrossRef]
10. Zhu, Z.; Pan, H.; Murugananthan, M.; Gong, J.; Zhang, Y. Visible light-driven photocatalytically active g-C_3N_4 material for enhanced generation of H_2O_2. *Appl. Catal. B Environ.* **2018**, *232*, 19–25. [CrossRef]
11. Hirakawa, H.; Shiota, S.; Shiraishi, Y.; Sakamoto, H.; Ichikawa, S.; Hirai, T. Au Nanoparticles Supported on $BiVO_4$: Effective Inorganic Photocatalysts for H_2O_2 Production from Water and O_2 under Visible Light. *ACS Catal.* **2016**, *6*, 4976–4982. [CrossRef]
12. Tsukamoto, D.; Shiro, A.; Shiraishi, Y.; Sugano, Y.; Ichikawa, S.; Tanaka, S.; Hirai, T. Photocatalytic H_2O_2 Production from Ethanol/O_2 System Using TiO_2 Loaded with Au–Ag Bimetallic Alloy Nanoparticles. *ACS Catal.* **2012**, *2*, 599–603. [CrossRef]
13. Cai, R.; Kubota, Y.; Fujishima, A. Effect of copper ions on the formation of hydrogen peroxide from photocatalytic titanium dioxide particles. *J. Catal.* **2003**, *219*, 214–218. [CrossRef]
14. Teranishi, M.; Naya, S.-I.; Tada, H. In Situ Liquid Phase Synthesis of Hydrogen Peroxide from Molecular Oxygen Using Gold Nanoparticle-Loaded Titanium(IV) Dioxide Photocatalyst. *J. Am. Chem. Soc.* **2010**, *132*, 7850–7851. [CrossRef]
15. Goto, H.; Hanada, Y.; Ohno, T.; Matsumura, M. Quantitative analysis of superoxide ion and hydrogen peroxide produced from molecular oxygen on photoirradiated TiO_2 particles. *J. Catal.* **2004**, *225*, 223–229. [CrossRef]
16. Hirakawa, T.; Nosaka, Y. Selective Production of Superoxide Ions and Hydrogen Peroxide over Nitrogen- and Sulfur-Doped TiO_2 Photocatalysts with Visible Light in Aqueous Suspension Systems. *J. Phys. Chem. C* **2008**, *112*, 15818–15823. [CrossRef]

17. Zheng, L.; Su, H.; Zhang, J.; Walekar, L.S.; Molamahmood, H.V.; Zhou, B.; Long, M.; Hu, Y.H. Highly selective photocatalytic production of H_2O_2 on sulfur and nitrogen co-doped graphene quantum dots tuned TiO_2. *Appl. Catal. B Environ.* **2018**, *239*, 475–484. [CrossRef]
18. Teranishi, M.; Naya, S.-I.; Tada, H. Temperature- and pH-Dependence of Hydrogen Peroxide Formation from Molecular Oxygen by Gold Nanoparticle-Loaded Titanium(IV) Oxide Photocatalyst. *J. Phys. Chem. C* **2016**, *120*, 1083–1088. [CrossRef]
19. Li, X.; Chen, C.; Zhao, J. Mechanism of Photodecomposition of H_2O_2 on TiO_2 Surfaces under Visible Light Irradiation. *Langmuir* **2001**, *17*, 4118–4122. [CrossRef]
20. Maurino, V.; Minero, C.; Mariella, G.; Pelizzetti, E. Sustained production of H_2O_2 on irradiated TiO_2—Fluoride systems. *Chem. Commun.* **2005**, *20*, 2627–2629. [CrossRef]
21. Liu, L.; Li, P.; Adisak, B.; Ouyang, S.; Umezawa, N.; Ye, J.; Kodiyath, R.; Tanabe, T.; Ramesh, G.V.; Ueda, S.; et al. Gold photosensitized $SrTiO_3$ for visible-light water oxidation induced by Au interband transitions. *J. Mater. Chem. A* **2014**, *2*, 9875–9882. [CrossRef]
22. Kosaka, K.; Yamada, H.; Matsui, S.; Echigo, A.S.; Shishida, K. Comparison among the Methods for Hydrogen Peroxide Measurements To Evaluate Advanced Oxidation Processes: Application of a Spectrophotometric Method Using Copper (II) Ion and 2,9-Dimethyl-1,10-phenanthroline. *Environ. Sci. Technol.* **1998**, *32*, 3821–3824. [CrossRef]
23. Jyothi, M.; Laveena, P.D.; Shwetharani, R.; Balakrishna, G.R. Novel hydrothermal method for effective doping of N and F into nano Titania for both, energy and environmental applications. *Mater. Res. Bull.* **2016**, *74*, 478–484. [CrossRef]
24. Jia, H.P.; Zhang, X.; Du, A.J.; Sun, D.D.; Leckie, J.O. Self-etching reconstruction of hierarchically mesoporous F-TiO_2 hollow microspherical photocatalyst for concurrent membrane water purifications. *J. Am. Chem. Soc.* **2008**, *130*, 11256–11257.
25. Mendez, F.J.; González-Millán, A.; Garcia-Macedo, J.A. A new insight into Au/TiO_2-catalyzed hydrogen production from water-methanol mixture using lamps containing simultaneous ultraviolet and visible radiation. *Int. J. Hydrogen Energy* **2019**, *44*, 14945–14954. [CrossRef]
26. Zuo, G.; Li, B.; Guo, Z.; Wang, L.; Yang, F.; Hou, W.; Zhang, S.; Zong, P.; Liu, S.; Meng, X.; et al. Efficient Photocatalytic Hydrogen Peroxide Production over TiO_2 Passivated by SnO_2. *Catalysts* **2019**, *9*, 623. [CrossRef]
27. Song, H.; Meng, X.; Wang, S.; Zhou, W.; Wang, X.; Kako, T.; Ye, J. Direct and Selective Photocatalytic Oxidation of CH_4 to Oxygenates with O_2 on Cocatalysts/ZnO at Room Temperature in Water. *J. Am. Chem. Soc.* **2019**, *141*, 20507–20515. [CrossRef] [PubMed]